AERODYNAMIC MODELLING OF SPACECRAFT FOR PRECISE ORBIT DETERMINATION

J Stark

Department of Aeronautics and Astronautics
University of Southampton
England

ABSTRACT

Examination is made upon the sensitivity of orbit prediction due to spacecraft aerodynamic forces. By separating the molecular momentum flux due to impinging and reemitted molecules, it is demonstrated that lifting forces are very much more sensitive to the model adopted for gas/surface interactions than the drag force experienced by a vehicle travelling in low earth orbit. An empirically based parametric model for gas/surface interactions is summarized and compared with thermal equilibrium and Schamberg models. The dominant effect of changing the interaction model is upon along track perturbations - decametric level. Radial purturbations are noted at the deci- and centimetric level. It is concluded that the only method available to reducing orbit determination residuals caused by aerodynamic forces, is through additional experimental data of gas/surface interactions.

Keywords: spacecraft aerodynamics, gas/surface interactions, precise orbit determination.

1. INTRODUCTION

The motion of a space vehicle in low earth orbit is subjected to a variety of perturbing forces, which result in the vehicle adopting a non-Keplerian orbit. In this orbit the most dominant of these forces results from the non-spherical, non-uniform mass distribution of the earth itself. These gravitational forces lead to the greatest modelling errors in the ability to determine a spacecraft orbit precisely. This feature was well demonstrated by the work on Seasat. However as was also noted for Seasat [Ref.1], for long arcs of 18 days duration, the problem of aerodynamic modelling leads to significant orbit determination errors.

Aerodynamic forces on spacecraft arise due to momentum exchange between atoms and molecules in the upper atmosphere and the vehicle itself. The magnitude of these forces is thus dependant upon both the incident momentum flux to a surface, and hence the number density of the atmosphere, and also the momentum flux of molecules and atoms leaving the surface of the vehicle. Evidently the instantaneous force is proportional to the local density at the satellite, and thus aerodynamic force modelling is dependant upon the model adopted for the earth's atmosphere. There are a large number of models of the atmosphere, which whilst differing in detail, provide similar gross features of the atmosphere. Indeed the primary differences under static conditions (modest solar activity and low geomagnetic activity) arise from differences in specific species concentration, and differences of absolute density; the overall morphological features (diurnal buldge etc.) remain remarkably constant for each of the atmospheric models. This may be seen most markedly in the work of Wakker et al.[Ref.5], wherein it was demonstrated that changing the atmospheric model does not produce the substantial effects on orbit determination accuracy which may be expected.

In principal therefore, the momentum flux incident upon a surface, may be reasonably well defined by adopting any one of a range of atmospheric models and then scaling the absolute value of force from the observed motion of the vehicle. This approach does not however solve the problem of the reflected momentum flux. In order to determine the component of force arising from molecular reflection, it is necessary to determine the velocity distribution function of the individual atmospheric components reflected from a surface. From the relatively few experimental results, this function is dependant upon the incident energy, the relative velocity and the type of species incident upon the surface, in addition to the surface material type. Characterisation of this momentum exchange is usually via the energy or momentum accommodation coefficients.

These coefficients must therefore either be predicted theoretically or evaluated experimentally in order to determine the momentum flux reflected from a surface. Detailed theoretical studies of examining gas surface interactions have produced very poor results [Ref.6] for accommodation coefficients, when compared with the limited experimental results. Many workers still rely therefore on the classical calculations of hard (or soft) sphere collisions.

The angular distribution of molecules reflected from the surface is dependant upon the interaction model. Two *"limiting"* cases may be referred to: diffuse reflection (cosine law) and specular reflections, however these models grossly simplify the situation. Nocilla [Ref.8], noted that the observed properties of the distribution function could not be met by a simple two component model, where part of the molecules were reflected specularly and part diffusely. Schamberg [Ref.9] parameterised the

Proceedings of the Second International Symposium on Spacecraft Flight Dynamics, Darmstadt, FR Germany, 20–23 October 1986 (ESA SP-255, Dec. 1986)

interaction in terms of three variables: alowing reflection to take place within a cone of specified half angle, dependant upon the angle of incidence between the surface and flow field, and the value for α. A limitation of this work is in the assumption that the incident flow field is hyperthermal, and thus the thermal velocity component is negligible in comparison to the flow velocity (i.e. space-craft orbital velocity). Whilst this is a reasonable approximation at low altitudes, above ~700km this approximation is inappropriate [Ref.7].

None of the above work has examined in any detail the influence of interaction model on orbit modelling accuracy. From the work performed on Seasat it is evident that aerodynamic forces vary around the orbit [Ref.1]. Whilst in part this is due to mis-modelling of atmospheric density changes, variation of aerodynamic coefficients should form an integral part of the modelling procedures. In this paper therefore examination is made into the sensitivity of orbit modelling to differing surface interaction models. Components of incident and reflected momentum are treated separately in this investigation in order to highlight these effects.

2. FREE-MOLECULE AERODYNAMICS

At orbitting spacecraft altitudes, the mean free path between atmospheric component collisions is typically very much larger than space vehicle characteristic dimensions. Modifications of the incident flow field due to the reflection of atmospheric components from a surface, may therefore be neglected in this free-molecular flow.

2.1 Incident Momentum Flux

Under free-molecular conditions and if one assumes the components of the flow are in thermodynamic equilibrium it is possible to write down the incident momentum flux on a surface element directly from kinetic theory. Referring to Figure 2, the incident momentum flux P_i normal to a surface element δA is given by:

$$P_i = \frac{\rho m \beta_0^3}{\pi^{3/2}} \int_{-\infty}^{+\infty} \int_{-\infty}^{+\infty} \int_{-c_o \cos\theta}^{\infty} \exp\left(-\beta_o^2 \omega^2\right) \exp\left(-\beta_o^2 v^2\right) \cdot \exp\left(-\beta_o^2 u^2\right) \cdot \left(u + c_o \cos\theta\right)^2 \, du \, dv \, d\omega \quad (1)$$

where u, v and ω are cartesian velocity components. β_o is the reciprocal of the most probable velocity, given by $\beta_o = (2RT)^{-\frac{1}{2}}$ where R is the gas constant for the particular gas and T the gas temperature. ρ is the gas number density and m the mass of each molecule.

By resolving P_i and a similar expression for shear stress, τ_i along the flow direction and normal to the flow direction it is possible to obtain the drag and lift coefficients due to the incident species upon integration over the surface of the body. For the simple case of a flat plate at an angle of incidence ϕ to the flow the drag and lift coefficients (C_D^i, C_L^i) are given by:

$$C_D^i = \frac{2}{\pi^{\frac{1}{2}} . s} . \exp\left(-s^2 \sin^2\phi\right) + 2\sin\phi\left(1 + \frac{1}{2s^2}\right) . erf\left(s . \sin\phi\right) \quad (2)$$

$$C_L^i = \frac{\cos\phi}{s^2} . erf\left(s . \sin\phi\right) \quad (3)$$

where s is the molecular speed ratio, being the ratio of flow bulk velocity, c_o, to most probable thermal velocity $1/\beta_o$. Since atmospheric composition and spacecraft velocity is a function of altitude, s is also a function of altitude. This dependance is shown, for circular orbits in Figure 1, for a COSPAR atmosphere (Ref.4).

It should be noted that these two expressions are valid only if the velocity distribution of atmospheric species is Maxwellian, however no assumption in these expressions has been made concerning hyperthermal flow.

2.2 Reflected Momentum Flux

The reflected momentum flux is, as stated earlier, dependant upon the velocity distribution function of the reflected species. This function is poorly determined, and thus it is appropriate to consider the influence of varying this function.

Assume that the velocity distribution function for reflected molecules of type j is given by f_j. Referring to Figure 3 which indicates a surface element whose outward normal is given by n, it is necessary to use f_j to evaluate the value of reflected molecule speed, c, as a function of the angle η (relative to n) and χ (relative to some arbitrary line in the plane of the element δA. (Use of the polar coordinate system makes the evaluation of reflected species fluxal quantities more straightforward than the cartesian set noted above).

By extension of equilibrium kinetic theory the reflected normal momentum flux of the reflected gas having number density ρ_R^j for species j, p_r^j is simply given by:

$$p_r^j = \int_0^{2\pi} \int_0^{\pi/2} \int_0^{\infty} \rho_R^j . m_j . c^4 . \sin\eta . \cos^2\eta . f_j . dc . d\eta . d\chi \quad (4)$$

and shear stress τ_r^j

$$\tau_r^j = \int_0^{2\pi} \int_0^{\pi/2} \int_0^{\infty} \rho_R^j . m_j . c^4 \sin^2\eta . \cos\eta . \cos\chi . f_j \, dc \, d\eta \, d\chi \quad (5)$$

Considering the expression for shear stress it should be noted that if f_j is independant of χ then the shear stress is zero. The physical interpretation of this is that the interaction between gas molecules and surface atoms is neither aligned to any surface conditions, nor to the incident direction and hence there can be no shear stress. The former condition is probable, since the surface of a spacecraft is effectively an engineering surface and thus the diffraction effects noted for pure crystalline surfaces

is most unlikely. The latter condition is more suspect in that it requires that molecules lose knowledge of their original direction during the interaction. Clearly the residence time of a molecule on a surface will be influential in this respect and it is therefore necessary to consider the sticking probability of a molecule to the surface.

In the altitude range of interest for most spacecraft applications, the dominant species is atomic oxygen. Indeed under conditions of high solar activity atomic oxygen can be dominant to altitudes in excess of 1000km [Ref.10]. Under modest solar activity conditions ($T_{exospheric}$ ~900°K) atomic oxygen contributes in excess of 30% of the momentum flux impinging on a surface at 800km, and it is only under the quietest periods of solar activity that atomic oxygen will contribute negligibly to the aerodynamic forces above ~ 500km.

The impact energy of oxygen (~5eV) is sufficient for chemisorption to take place [Ref.7]. Indeed the recent evidence from shuttle experience [Ref.11] showing marked erosion rates would support this. For such reactions to take place, a significant residence time would be inferred. Therefore in respect of atomic oxygen it seems plausible to assume that the function f_j is uncorrelated with χ.

We may thus assume that f_j is a function of η and the surface temperature only. Assuming chemisorption does take place it is then necessary to consider molecular desorption from the surface. There is considerable evidence from desorption studies [Refs 12 and 13] that desorption is not a diffuse process, in that the differential number flux may be approximated by a function of the form $\cos^r(\eta)$ Further the effective temperature of desorbed atoms has also been shown to be a function of χ [Refs.12 and 14]. There are two solutions which may therefore be arrived at: either there is a net velocity component of molecules away from the surface (effectively the Nocilla solution [Ref.8]) or the molecules do not have such a streamwise component.In view of the evidence for variation of molecular temperature with η it seems more appropriate to consider this latter possibility in greater detail.

Consider an analytic function $A.f_j'(\eta, T)$ where A is the normalisation coefficient for the probability function f_j'. On this basis, the molecular velocity distribution may be considered to arise from a stationary gas whose temperature is dependant upon the angle that the molecule's velocity vector makes with the surface normal n. Evidence for this dependance is demonstrated by the experimental data of Cosma [Ref.12]. This data suggests that the temperature of re-emitted molecules may be written in the form:

$$T(\eta) = T_o(1 + b\cos\eta) \tag{6}$$

T_O is a reference temperature and b is a constant, which may be used to fit the data.

It is now possible to arrive at an appropriate form for the reemission velocity probability distribution function. If this function is assumed to be a modified Maxwellian then we may rewrite $f_j'(\eta, T)$ as $P_j(\eta).\exp(-\beta^2c^2)$ and thus the number flux from the surface is given by:

$$N_j^R = \rho_R^j \int_0^{\pi/2}\int_0^{2\pi}\int_0^{\infty} AP_j.c^3 exp(-\beta^2c^2).\sin\eta\cos\eta\,.\,dc\,.\,d\chi\,.\,d\eta \tag{7}$$

β is found from Eqn.6,and assumes that the speed distribution of gas molecules at a given temperature is Maxwellian.

Performing the integral over the first two inner terms yields

$$N_j^R = \rho_R \int_0^{\pi/2} A.\frac{P_j(\eta)}{2\beta^4}\,.\sin\eta\cos\eta\,d\eta \tag{8}$$

But the experimental evidence noted above suggests that the probability of the number flux lying between η and $\eta + \Delta\eta$ is of the form $\cos^r\eta$. Thus if this function is given by $N_j(\eta)$, we require

$$N_j(\eta) = B\cos^r\eta = A.\frac{P_j(\eta)}{2\beta^4}\,.\sin\eta\cos\eta\,d\eta \tag{9}$$

The functional form of this condition can be met with

$$P_j(\eta) = \beta^4.\cos^{r-2}\eta. \tag{10}$$

The value for A can be determined from the unity condition, namely the probability of finding a molecule on the positive side of the plate is one. The velocity distribution function is thus:

$$f_j = A.f_j'(\eta,T) = A.\beta^4\cos^{r-2}\eta.exp(-\beta^2c^2) \tag{11}$$

where β is obtained through Eqn.6 for a maxwellian.

It is now possible to evaluate the momentum flux normal to a surface element by evaluating the integral of Eqn.11; before doing so it is important to note that the reflected number density of the gas is not equal to the incident number density. Assuming continuity at the surface, and thus neglecting surface chemistry which may result in chemical sputtering, it is possible to equate the flux of molecules impacting on the surface to the flux reemitted. If we assume that there is only one component to the gas (neglect the generalized j notation), a single expression may be used to describe the gas. The flux reemitted has already been defined through Eqn.7. A similar expression for the incident flux based on a maxwellian gas with stream speed to thermal speed ratio of s, on integration yields:

$$P_R = \frac{\rho_i.r}{2\pi^{3/2}A\beta_i}\left[exp\left(-s^2.\cos^2\theta\right) + \pi^{\frac{1}{2}}s.\cos\theta\left[1+erf\left(s.\cos\theta\right)\right]\right] \tag{12}$$

where β_i is the β value for the incident gas stream. On substituting Eqn.12 into Eqn.4, the reflected momentum flux in terms of the incident stream number density may be obtained.

These expressions may then be used to evaluate the drag and lift coefficients due to the reemission of molecules from a surface. It should be noted that these expressions reduce to the classical thermal values given by Stalder and Zurich [Ref.15] for diffuse reflection if b = 0 and r = 2 . Two further limiting cases are of interest. Firstly if b = 0, that is all molecules are reemitted at the same temperature T_o, then the reemission drag for a plate at an angle of attack α is:

$$C_D' = \frac{3}{2}.\frac{r}{r+1}.\left(\frac{T_o}{T_\infty}\right)^{\frac{1}{2}}.\frac{\pi^{\frac{1}{2}}.sin^2\alpha}{s} \qquad (13)$$

where T_∞ is the temperature of the free stream. In Eqn. 13 it is appropriate to note that contributions to the aerodynamic forces arise from both the upper and lower surfaces of the plate.

The corresponding value for the lift coefficient for the case of b = 0, due to reflected molecules is given by:

$$C_L' = \frac{3}{2}\frac{r}{r+1}.\left(\frac{T_o}{T_\infty}\right)^{\frac{1}{2}}\frac{\pi^{\frac{1}{2}}sin\alpha cos\alpha}{s} \qquad (14)$$

The second case of interest is found when r tends to infinity in Eqns.13 and 14, corresponding to an infinitely narrow reflected beam of molecules, emitted perpendicular to the surface at a temperature T_o. This may be likened to a pseudo specular reflection from the surface. Under these conditions the value for the drag and lift coefficients are 50% larger than for corresponding diffuse reemission.

3. NUMERICAL EXAMPLES

The example of a flat plate noted above is particularly relevant when considering 3-axis stabilized vehicles having large planar appendages such as solar arrays and synthetic apperture radar systems. Since these components are of large area, their aerodynamic characteristics will dominate the aerodynamic nature of such vehicles. It is therefore appropriate to investigate the aerodynamic forces on a flat plate as a function of the gas/surface interaction model. In this respect there are two features of particular relevance: the absolute value for C_D and the ratio of C_L/C_D. Relatively little attention in the past has been given to C_L, primarily since for most conditions the lift force is much less than the drag force [Ref.2]. However, as recently noted [Ref.3], under certain conditions lifting effects do become significant.

The expressions derived above may be used to give the total values of lift and drag coefficients, by summing incident and reflected momenta values.

For the generalized model given above, and assuming that the gas incident upon the plate only consists of a single component, then at an angle of attack ϕ, the values for C_D and C_L may be written:

$$C_D = \frac{2}{\pi^{\frac{1}{2}}.s}.exp(-s^2sin^2\phi)+2sin\phi\left(1+\frac{1}{2s^2}\right)erf(s.sin\phi) + .\pi^{\frac{1}{2}}\frac{sin^2\phi}{s}\left(\frac{T_o}{T_\infty}\right)^{\frac{1}{2}}.\kappa \qquad (15)$$

and

$$C_L = \frac{cos\phi}{s^2}.erf(s.sin\phi)+.\pi^{\frac{1}{2}}.\frac{sin\phi cos\phi}{s}.\left(\frac{T_o}{T_\infty}\right)^{\frac{1}{2}}.\kappa \qquad (16)$$

where

$$\kappa = 1.5.r.\left\{\frac{1}{r+1}+\frac{b}{2(r+2)}-\frac{b^2}{8(r+3)}+\ldots \frac{(-1)^m b^{m-1}3.5\ldots(2m-5)}{2^{m-1}.(m-1)!(r+m)}+..\right\} \quad for\ |b|<1$$

and

$$\kappa = \frac{3.r.r!}{b^{r+1}}\left[\sqrt{1+b}\sum_{m=0}^{r}\frac{(-1)^{r-m}(1+b)^{m+1}}{m!(r-m)!(2m+3)}-\sum_{m=0}^{r}\frac{(-1)^{r-m}}{m!(r-m)!(2m+3)}\right] \quad for\ |b|>1$$

With regard to these expressions, it is notable that the reflected momentum component to lift and drag is simply obtained by including a scaling factor relative to a thermal diffuse reflection model for the gas/surface interaction. It is therefore appropriate to consider first the ratio of reflected to incident momenta contributions under conditions of thermally diffuse reflection. In Figure 4, the ratio of reflected to incident lift components is plotted as a function of angle of attack, ϕ, for various speed ratio values. Figure 5 plots similar results for drag components.

In comparing these two figures it is apparent that lift is very much more sensitive to the reflected component of momentum, than is drag. Indeed under all conditions plotted in Figures 4 and 5, the ratio of reflected incident momentum for lift is more than an order of magnitude greater than that for drag. This evidently implies that lift forces are more sensitive to the model adopted for the gas/surface interaction than is the case for drag forces. This sensitivity is more pronounced for flow fields having high speed ratios; that is to say at low altitudes (see Figure 1).

Figure 6 demonstrates the variation of the scale factor κ, as a function of both r (the *"peakiness"* of the reflection distribution) and b (the degree of non-uniformity in reemission temperature). From this figure it is apparent that κ is relatively insensitive to the value of r, although as would be expected greater effect is noted for a large temperature spread in reemitted molecules. However, even with high values of b, little variation of κ occurs for values of r in excess of ~8. The magnitude of κ is most sensitive to the value of b. It is therefore most important that the temperature distributions noted in [Ref.19] be investigated for species and surfaces appropriate to the spacecraft environment.

Figure 7 compares lift/drag ratios as a function of ϕ for two well known models - the Schamberg diffuse model and the classical diffuse model (in our case corresponding to r = 2, b = 0). This figure shows a substantial difference in predicted aerodynamic properties, particularly at low angles of attack (a condition particularly pertinent when considering SAR antennas).

Figures 8 and 9 show results for L/D ratios and C_D values for the more generalized model of surface accommodation described in Section 2; for low speed ratio, in Figure 8, appropriate for high altitude orbits (~800km) and high speed ratio (Figure 9), appropriate at a lower altitude (~300km). The important features to note from these figures are the following:

i) The absolute value of C_D is more sensitive to the surface model adopted at high angles of attack than at low angles of attack; enhanced sensitivity to the interaction model is also noted at low speed ratio (i.e. high altitude operation).

ii) The lift to drag ratio is always greater for the model described in Section 2, than the classical thermal diffuse reflection model, except at zero and perpendicular incidence angles.

iii) In comparing the lift to drag ratios for small and large speed ratios, it may be noted that the latter case (i.e. low altitude) is slightly more sensitive to the surface model adopted.

In summary it should be noted that parameterising the surface interaction model on the basis of the observational evidence, into an appropriate analytic expression, demonstrates the complex relationship not only between drag and lift to drag ratios, but also the relationship with the altitude of the vehicle and vehicle type. It is therefore appropriate to consider a specific example of a vehicle, to establish orbit sensitivity to the interaction model adopted.

4. ORBITAL SENSITIVITY ANALYSIS

In order to examine the influence of the adopted gas surface interaction model upon orbit prediction, the parametric model described above was used to investigate the orbit prediction sensitivity for an ERS 1 type vehicle.

The model vehicle was assumed to consist of 3 major components: a $20m^2$ solar array (always sun pointing), an $11m^2$ synthetic aperture radar (pointing in a specified manner) and a $5m^2$ cube type body (pointing in a specified manner). The gas-surface model described above, together with the classical thermal diffuse model and hyperthermal Schamberg model were all investigated for comparison purposes.

The atmosphere through which the vehicle was assumed to move was a synchronously rotating COSPAR atmosphere under conditions of varying solar activity [Ref.14]. The incident speed ratio of the impinging atmosphere was computed on the basis of the mean molecular weight calculated at each position of the orbit evaluation procedure.

The equations of motion for predicting the vehicle trajectory were obtained using Lagrange's planetary equations.

These equations were solved numerically by adopting Merson's Runge-Kutta method of integration. For the purposes of these comparisons a pointlike earth gravity model was adopted to highlight the specific influences of the aerodynamic force vector.

Orbital sensitivity to parameter variation was determined by evaluating the radial, along track and cross track purturbations over one orbit. These are given to order (e) by [3]:-

$$\Delta r = \Delta a - a\Delta e$$

$$\Delta \ell = a(\Delta M + \Delta\omega + \Delta\Omega \cos i)$$

$$\Delta c = a(\Delta i \sin\omega - \Delta\Omega \sin i \cos\omega)$$

The baseline orbit taken for ERS1 [Ref.5] has the following orbital parameters: a = 7153.1439km, e = 0.001, i = 98°.52146, Ω = 247°.069; ω = 90°.00.

Firstly, considering the variation of aerodynamic forces around a single orbit, Figure 10 shows force as a function of true anomaly θ. Curves are shown for both the thermal and Schamberg models together with the variable reemission model described above. For the variable re-emission model, the values of κ were chosen to be 2.0, 5.0 and 10.0. Specific values of κ were selected in preference to values for r and b, due to the non-unique values of these parameters for specifying a value for κ.

In Figure 10 it is apparent that in general terms the shape of the force function is fairly similar for all of the models indicated. As would be expected increasing κ increases the total force, however it is also noticable that the detailed variation of force around the orbit is indeed dependant upon the re-emission model. Since the drag force is very much greater than the lifting forces, and as noted above the drag force is relatively insensitive to re-emission model, these results are not surprising.

Figure 11 shows the lift/drag ratio values for the same condition as Figure 10. Here significant changes with the re-emission model are seen. Not only does the magnitude of this ratio depend critically upon the model adopted, but also the general shape of this ratio around the orbit, is influenced. This implies that if lift effects are to be included in P.O.D. analysis, then it is inappropriate to solve for C_L, as is frequently done for C_D in orbit determination studies.

The influence of these parameters on orbit determination can be seen in Figures 12 to 14. These highlight the sensitivity of orbit evolution to the changing orientation of the relative spacecraft components. Values are shown for changing values of

Ω, having a major influence on the orientation of the solar array. For each of these plots the S.A.R. was assumed to point to the nadir.

The results presented in Figures 12 to 14 show the change in Δr, $\Delta \ell$ and Δc for a specific re-emission model relative to a thermally accommodated diffuse re-emission model. A nominal average solar activity level ($F_{10.7} = 175$, $K_p = 0$) was assumed for atmospheric density/constituent prediction. From these results it is evident that the along track perturbation is most sensitive to variation in the re-emission model, with values approaching 18m when comparing a κ of 5 relative to the thermally accommodated model. Whilst cross track variations appear minimal for the models investigated, the orbit radial sensitivity is at the centimetre level. This radial sensitivity is further demonstrated in Figure 15, showing the influence of changing solar activity upon Δr. Clearly both Schamberg and Thermal models produce fairly consistent results at all values of $F_{10.7}$. This is not the case however for variable K type model.

5. CONCLUSIONS

From the results presented here it is apparent that the re-emission model adopted for gas/surface interactions can produce significant variation in orbital parameters. Whilst no preferred re-emission model is proposed here, it is apparent that for P.O.D. evaluation the variability of aerodynamic forces around an orbit should be included in analysis to reduce residuals. This leads inevitably to the conclusion that without additional appropriate experimental data on gas surface interactions, reduction in errors arising from mis-modelling of the aerodynamic properties of spacecraft may not be achieved.

REFERENCES

[1] Schultz, B.E. and Tapley, B.D., Orbit Accuracy Assessment for Seasat, J. Astron Sci Vol 28, pp371-390, 1980.

[2] King Hele, D.G., "Theory of satellite orbits in an atmosphere" pb Butterworths 1964.

[3] Moore, P., The effects of aerodynamic lift of near circular orbits, Pl.Sp.Sc. Vol 33, pp479-491, 1985.

[4] CIRA; COSPAR International Reference Atmosphere 1972, Compiled by members of the Cospar Working Group IV, Published by Pergamon Press 1972.

[5] Wakker, K.F., Ambrosius, B.A.C. and Aardoom, L., Precise Orbit Determination for ERS-1, ESOC contract 5227/82/D/iM(SC), 1983.

[6] Goodman, F.O. and Wachman, H.Y., Dynamics of Gas-Surface Scattering, Published by Academic Press, 1976.

[7] Cook, G.E., Satellite Drag Coefficients, Pl Sp.Sc. Vol 13, pp929-946, 1965.

[8] Nocilla, S., Theoretical Determination of Aerodynamic forces on Satellites, Acta Astronautica, Vol 17, pp245-258, 1972.

[9] Schamberg, R., Rand Research memorandum RM-2313, 1959.

[10] Jacchia, L.G., Revised Static Models of the thermosphere and exosphere with empirical temperature profiles, SAO special report 332 (1971).

[11] Whitaker, A.F., Little, S.A., Harwell, R.J., Gnner, D.B., De Haye, R.F. and Fromhold, A.T., Orbital Atomic Oxygen Effects on Thermal Control and optical materials STS8 Results, AIAA Paper 85-0416, 1985.

[12] Cosma, G., D. Rudolf and B.J. Schumacher, "The angular dependence of flux, mean energy and speed for D_2 molecules desorbing from a Ni(111) surface". Surface Science 85, pp45-68, 1979.

[13] Halpern, B. and Rosner, D.E., 'Incomplete Energy Accommodation in Surface Catalysed reactions', Heterogenous Atmospheric Chemistry, Geophysical Monograph Series American Geophysical Union pp167-172, 1982.

[14] Tulley, J.F., "Dynamics of gas-surface interactions: Reaction of atomic oxygen with absorbed carbon on platinum", J. Chem. Phys 73, pp6333-6342, 1980.

[15] Stalder, J.R. and V.J. Zurich, NACA TN-2423, 1951.

[16] See Special Edition of J. Astron Sci., ref.[1].

FIGURES

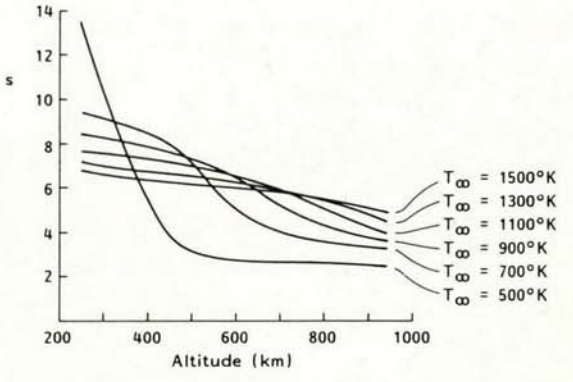

FIG. 1 VARIATION OF SPEED RATIO s AS A FUNCTION OF ALTITUDE AND T_∞

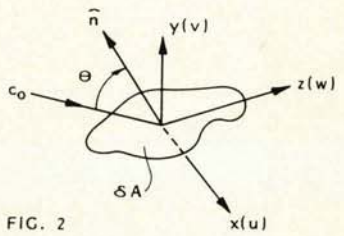

FIG. 2

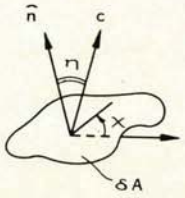

FIG. 3

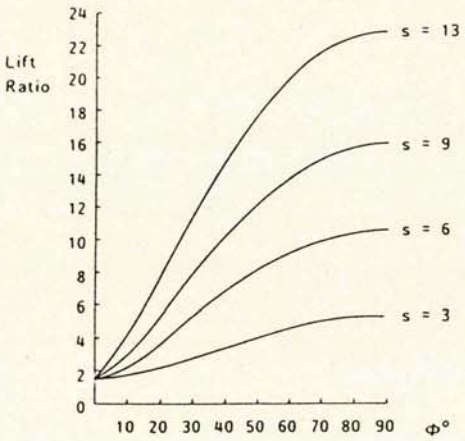

FIG. 4 RATIO OF REFLECTED : INCIDENT MOMENTUM CONTRIBUTING TO LIFT.

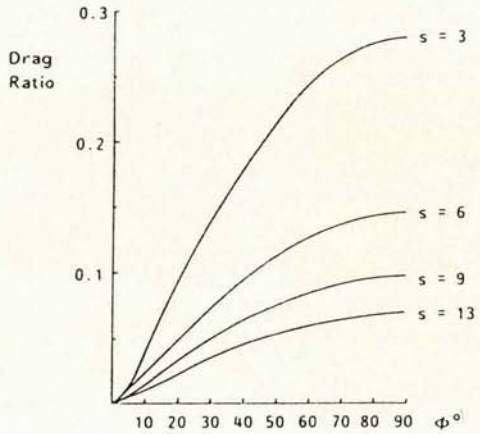

FIG. 5 RATIO OF REFLECTED : INCIDENT MOMENTUM CONTRIBUTING TO DRAG.

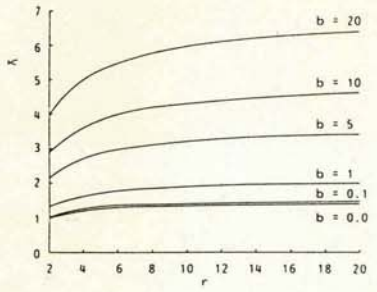

FIG. 6 VARIATION OF κ WITH b AS A FUNCTION OF r

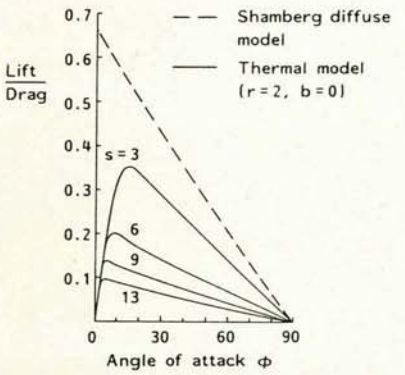

FIG. 7 VARIATION OF LIFT:DRAG RATIO FOR $T_o / T_\infty = 1$

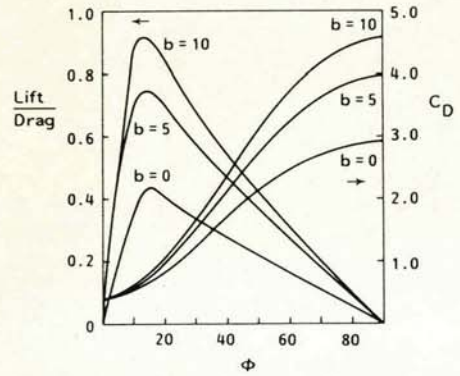

FIG. 8 LIFT/DRAG RATIOS AND C_D FOR SPEED RATIO s = 3.0 AND r = 8

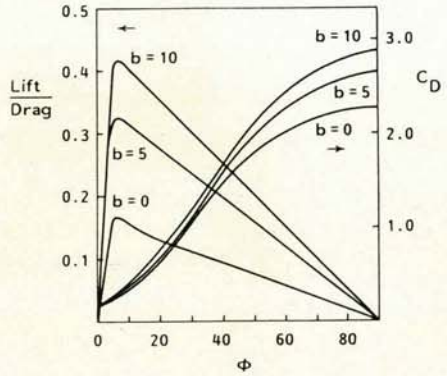

FIG. 9 LIFT/DRAG RATIO AND C_D FOR SPEED RATIO s = 9.0 AND r = 8

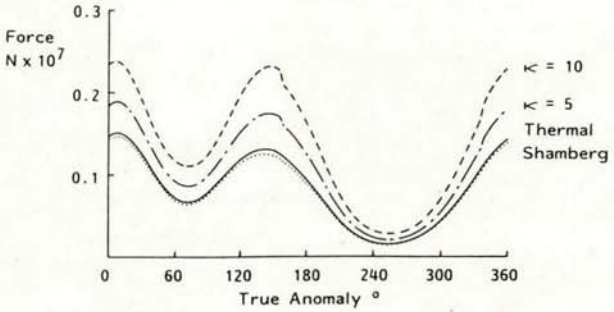

FIG. 10 FORCE VARIATION AROUND ORBIT

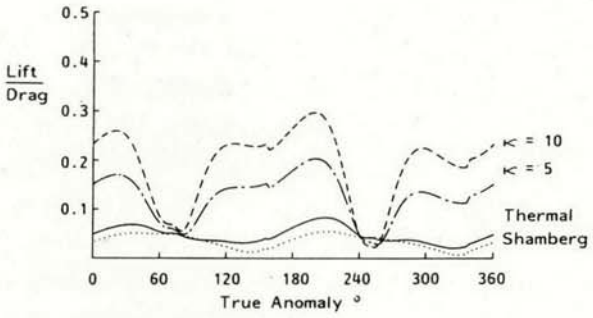

FIG. 11 L/D RATIO VARIATION IN ONE ORBIT

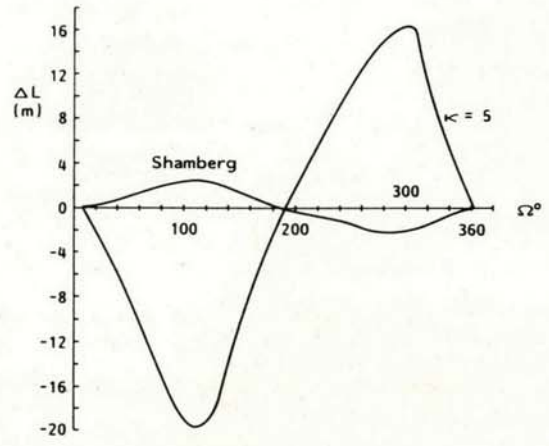

FIG. 12 ALONG TRACK PERTURBATION IN m RELATIVE TO THERMAL EQUILIBRIUM MODEL.

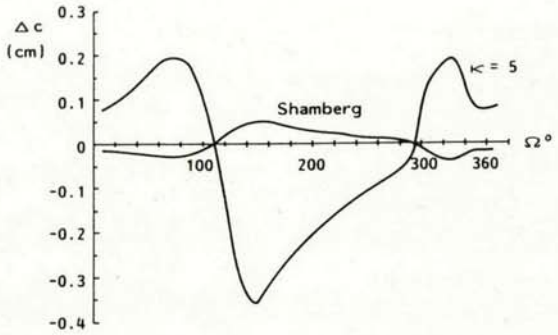

FIG. 13 CROSSTRACK PERTURBATION IN cm RELATIVE TO THERMAL EQUILIBRIUM MODEL.

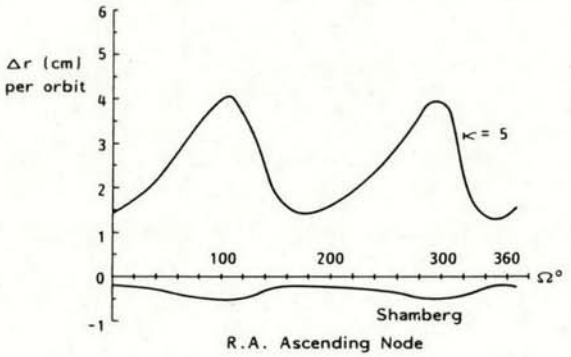

FIG. 14 RADIAL PERTURBATION IN cm RELATIVE TO THERMAL EQUILIBRIUM MODEL.

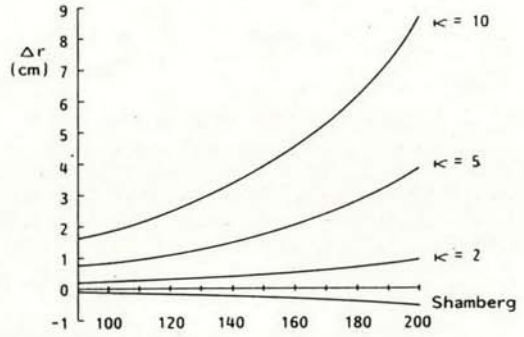

FIG. 15 Δr SENSITIVITY TO SOLAR ACTIVITY RELATIVE TO THERMAL RE-EMISSION MODEL.